



Numerical Study of Turbulent Airflow Structure and Transfer of Heat Having Trapezoidal Baffles Attached on the Walls and Centerline of the Rectangular Channel

Sandip Saha¹ · Pankaj Biswas² · Apurba Narayan Das³

Accepted: 17 January 2022 / Published online: 15 April 2022

© The Author(s), under exclusive licence to Springer Nature India Private Limited 2022

Abstract

Numerically, we have studied different characteristics of turbulent air flow (flow structure, axial velocity profiles, dimensionless coefficient of skin friction, normalized friction factor), and heat transfer (local Nusselt number, and average Nusselt number) phenomena through a rectangular channel having trapezoidal baffles attached on its walls, and along the centerline of it. The governing equations have been solved using the finite volume method and to visualize the simulation results, fluent software has been employed. It is shown that the maximum value of pressure drop occurs on the upstream, and minimum value attains in the downstream section of the channel. It is ensured that an increase in the Reynolds number (Re) causes increase in normalize friction factor (F), and average Nusselt number (Nu_{av}). The simulation results of this work will help to design and monitor flow phenomena through many thermal applications.

Keywords Rectangular channel · Turbulent flow · Baffles · Absolute pressure drop

List of Symbols

C	Empirical constant, $C_\mu = 0.09$, $C_{1\epsilon} = 1.44$, $C_{2\epsilon} = 1.92$, $\sigma_k = 1.0$, $\sigma_\epsilon = 1.3$
C_p	Average pressure coefficient
$C_{f(x)}$	Skin friction coefficient
f_0	Friction factor of smooth channel [Petukhov[1]] = $(0.79 \ln Re - 1.64)^{-2}$ for $\leq Re \leq 500,000$
F	Average friction factor = $\frac{2\Delta p H}{L\rho u_0^2}$
F	Normalize friction factor = $\frac{f}{f_0}$

✉ Sandip Saha
sandip.tfgss@gmail.com

¹ Department of Mathematics, Madanapalle Institute of Technology and Science, Madanapalle, Andhra Pradesh 517325, India

² Department of Mathematics, National Institute of Technology Silchar, Silchar, Assam 788010, India

³ Department of Mathematics, Alipurduar University, Alipurduar, West Bengal 736121, India

G_k	Production rate of kinetic energy due to
$h(x)$	Coefficient of heat transfer
H	Channel width (m)
HT	Heat transfer
k_f	Thermal conductivity ($Wm^{-1} K^{-1}$)
k	Turbulent kinetic energy = $\frac{1}{2}u'_i u'_j$
L	Length of channel
M	Meter
N_e	Total number of elements
p	Pressure
p_1	Pressure at inlet
p_2	Pressure at outlet
Δp	Absolute pressure drop = $ (p_2 - p_1) $
T	Temperature
T_w	Wall temperature = 375 K
u'_i, u'_j	Fluctuation velocity components in x_i and x_j directions
u_0	Input velocity [ms^{-1}]
ρ	Density ($kg m^{-3}$)
μ	Dynamic viscosity [Pa.s]
Re	Reynolds number = $\frac{u_0 \rho H}{\mu}$
Nu	Nusselt number
$Nu(x)$	Local Nusselt number = $\frac{h(x)L}{k_f}$
Nu_{av}	Average Nusselt number = $\frac{1}{L} \int_0^L Nu(x) dx$
Nu_0	Average Nusselt number of smooth channel [Dittus and Boelter [2]] = $0.023Re^{0.8} Pr^{0.4}$ for $Re \geq 10,000$
Nu_{na}	Normalized average Nusselt number
$NC_f(x)$	Normalize skin friction coefficient = $C_f(x)/f_0$
FVM	Method of finite volume
Pr	Prandtl number
$\frac{\mu}{\rho r}$	Molecular diffusivity
$\frac{\mu_t}{\rho r}$	Turbulent thermal diffusivity
μ_t	Turbulent viscosity = $\rho C_\mu \frac{k^2}{\epsilon}$
δ_{ij}	Kronecker delta
Y^+	Normalize distance of the walls
k_p	Kinetic energy of turbulence at position P
y_p	Distance from position P to the wall
E	= 9.81
r	= 0.42
v	Velocity in y direction
x	Y, Cartesian coordinate
u_i	U_j , components of mean velocity [ms^{-1}] in x_i and x_j directions
T_{in}	Inlet temperature = 300 K

Introduction

Turbulent flow through a rectangular channel embedded with baffles has wide applications in many engineering equipment's like solar, chemical reactors etc. To produce shell and tube heat exchanger models, baffles play a crucial role. In a rectangular channel embedded with baffles, Wiemer [3] has investigated the flow turbulence, heat exchange ratios, and concluded that separation of boundary layer has greatly affected by the presence of baffles. To reveal the linear relationship between Re and Nu , Gunter et al. [4] have considered the flow visualization in presence of two staggered baffles. Latter on many authors [5–9] have extended their investigations considering pressure drop characteristics. Patankar [10] has studied the hydrothermal phenomena of fluid flow through a rectangular channel with plane baffles numerically. They revealed that the value of Nu_{av} increases due to the increase in Re . With staggered baffles, Bermer et al. [11] have experimentally studied mean velocity and turbulence distributions. Webb et al. [12, 13], Habib et al. [14, 15], Atabi (a,b) et al. [16, 17], Bazdidiet al. [18], Kelkar et al. [19], Prusty et al. [20], Saha et al. [21], Chhanda et al. [22], and Barik et al. [23] have numerically solved the problem on different characteristics of thermo-hydraulic flow phenomena over a rectangular channel with staggered baffles.

In a 3-D rectangular channel, embedded with baffles on its walls, Prithviraj et al. [24] have applied fully implicit control-based method to simulate the flow, and pressure drop characteristics. In different locations, they have studied the pressure drop properties. Moreover, they have revealed that the rate of HT increases significantly due to the presence of baffles. Over a rectangular channel with solid and perforated baffles, Prashanta et al. [25] have studied the different HT characteristics and the coefficients of frictional heat loss experimentally. They have deduced a linear relationship between Re , and pressure drop. Shavian et al. [26] have considered the problem of turbulent flow and dissipation rate for $Re \in [1-20, 20-37]$ through a square channel with or without baffles. Kang et al. [27] have showed that the presence of baffles increases the heat transfer rate by 300%. For a wide range of Re , Behera et al. [28] have studied the thermal enhancement in a three-dimensional rectangular duct. They have concluded that the value of Nu_{av} , I_p , and P_p increases with the increase of Re . Karwa et al. [29] have observed that the value of Nu is enhanced by 169% for the presence of fully perforated baffles/ribs. Bhuiya et al. [30] have deduced that the values of Nu_{av} and F are enhanced by 110%-340% and 110%-360%, respectively, due to the presence of the perforated baffles. For different values of Re , Barik et al. [31] have studied the thermo-hydraulic phenomena of cross-flow in a 3D small rectangular channel of different protrusion shapes (rectangular, trapezoidal and triangular). They have revealed that in the case of triangular protrusions, the rate of heat transfer becomes high as compared to the other protrusion shapes. In presence of protrusions, Mukherjee et al. [32] have investigated the enhancement of heat transfer and entropy generation over a rectangular duct numerically. They have concluded that the value of Nu_{av} enhances with the increase in Re . Using FVM, Mukherjee et al. [33] have investigated the different characteristics of thermo-hydraulic phenomena of mean flow through a rectangular channel with different protrusion surfaces (triangular and trapezoidal). They have studied the enhancement of heat transfer in both the cases of cross-flow and non-cross-flow. They have found that the cross-flow effect becomes more pronounced than the case of non-cross flow. In addition, it has been found that among all the protrusions, triangular protrusion is much more significant than other considered cases.

The relevant cited articles ensure that most of the studies are based on plane and ribbed baffles, and no study on the characteristics of hydrothermal turbulent flow phenomena having trapezoidal baffles attached along the wall and centerline on the channel has been made until

the date. Therefore, what would be the characteristics of velocity and pressure profiles, dimensionless coefficient of $C_f(x)$ and Nu_{av} , are remain as matter of interest. This work is an extension of the experimental and numerical works of Demartini et al. [34], where they have considered turbulent airflow phenomena in the presence of plane baffles without considering the heat transfer phenomena. The current work is confined in finding five characteristics of flow phenomena such as turbulence of flow, velocity and pressure profiles, coefficient of normalize $C_f(x)$, F , and to calculate the $Nu(x)$ and Nu_{av} for a wide range of Re lies between [1–12, 12–37]. The outcomes of this work will help to design, optimize and monitor flow phenomena through many thermal applications.

Problem Statement

To model the geometry and for simulation purpose, FLUENT [1–15] software has been employed. Figure 1 presents the rectangular channel with trapezoidal baffles attached on the walls and along the centerline of the channel. A constant surface temperature (T_w) has been assigned at the upper wall, and the lower wall has been kept insulated. The present work is based on the computational airflow dynamics over a rectangular channel with trapezoidal baffles. Needless to say that this model has applications in various engineering equipments, such as solar collectors and in aerospace industry [Habib et al. [14, 15], Atabi (a,b) et al. [16, 17], Bazdidi et al. [18]]. It is well known that the enhancement of heat transfer can be achieved by creating longitudinal vortices in the flow generated by the flat detached and attached baffles. The following assumptions have been made to carry out this work following the experimental and numerical studies of Demartini et al. [34], numerical works of Nasiruddin et al. [35], and Saha [37]:

- The flow is two-dimensional, incompressible, Newtonian, and steady-turbulent.
- The effects of radiation, viscous dissipation and body force are negligibly small. Here, viscous dissipation effects are neglected, as turbulence reduces the viscous effects at a distance from the solid boundary. Secondly, the Reynolds number is too high (that means inertia force much more significant than viscous force).
- The physical characteristics of air has been taken into account following the experimental and numerical works of Demartini et al. [34], and the numerical work of Nasiruddin et al. [35].

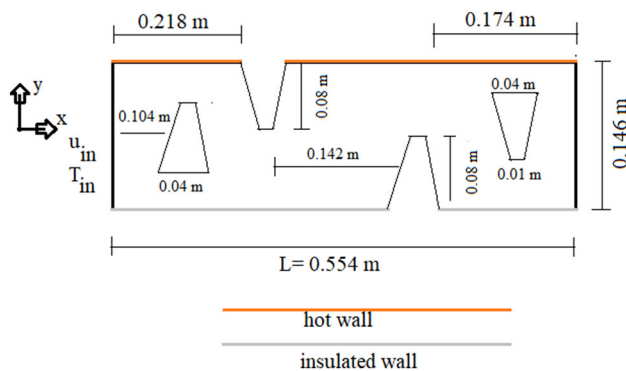


Fig. 1 Rectangular channel embedded with detached and attached trapezoidal baffles

Governing Equations

Following the experimental and numerical work of Demartini et al. [34] and the numerical work of Nasiruddin et al. [35], the present work studies the different characteristics of turbulent air flow and heat transfer phenomena which are governed by the continuity (Eq. 1), momentum (Eq. 2), and energy (Eq. 3) equations given below:

The continuity equation

$$\frac{\partial(\rho \cdot u_j)}{\partial x_j} = 0 \tag{1}$$

The momentum equation

$$\rho u_j \frac{\partial(u_i)}{\partial x_j} = -\frac{\partial p}{\partial x_i} + \frac{\partial}{\partial x_j} \left[(\mu + \mu_t) \frac{\partial u_i}{\partial x_j} + \mu_t \frac{\partial u_j}{\partial x_i} - \frac{2}{3} \rho \delta_{ij} k \right] \tag{2}$$

The energy equation

$$\rho u_j \frac{\partial T}{\partial x_j} = \frac{\partial}{\partial x_j} \left[\left(\frac{\mu}{Pr} + \frac{\mu_t}{Pr_t} \right) \frac{\partial T}{\partial x_j} \right] \tag{3}$$

As per the studies of Demartini et al. [34], the expressions of Y^+ and U^+ are:

$$Y^+ = \frac{\rho C_\mu^{1/4} k_p^{1/2} y_p}{\mu} \tag{4}$$

$$U^+ = \frac{\ln(EY^+)}{r} \tag{5}$$

in addition, the values of Y^+ and U^+ are taken as 35 and 13.90 respectively.

Standard k-ε Model

To study the flow behaviour and heat transfer characteristics, standard k- ε model [Lauder et al. [36]] has been used, which consists of two equations, as below:

Turbulent kinetic energy k:

$$\rho u_j \frac{\partial k}{\partial x_j} = \frac{\partial}{\partial x_j} \left[\left(\mu + \frac{\mu_t}{\sigma_k} \right) \frac{\partial k}{\partial x_j} \right] + G_k - \rho \epsilon \tag{6}$$

Dissipation rate ε:

$$\rho u_j \frac{\partial \epsilon}{\partial x_j} = \frac{\partial}{\partial x_j} \left[\left(\mu + \frac{\mu_t}{\sigma_\epsilon} \right) \frac{\partial \epsilon}{\partial x_j} \right] + C_{1\epsilon} \frac{\epsilon}{k} G_k - C_{2\epsilon} \frac{\epsilon^2}{k} \rho \tag{7}$$

Boundary Conditions

The hydrodynamic boundary conditions have been specified following the experimental works of Demartini et al. [34], and the thermal boundary conditions have been chosen from the work of Nasiruddin et al. [35] as.

- Inlet boundary condition: At $x = 0$, $u = u_0$, $v = 0$, $k_{in} = 0.005u_0^2$, $\epsilon_{in} = 0.005k_{in}^2$, $T = T_{in} = 300$ K.
- Outlet boundary condition: At $x = L$, the pressure boundary conditions require static gauge pressure, and in this case pressure at the outlet has been taken with zero gauge pressure ($\frac{\partial u_i}{\partial x_i} = 0$).
- Wall boundary conditions: $u = 0$, $v = 0$, $k = 0$, $\epsilon = 0$. At the upper wall $T_w = 375$ K, while the lower wall was thermally insulated.

Grid Test, Code Validation and Numerical Procedure

To reduce the computational cost and to identify the optimal grid, grid test has been done. The discretization of steady governing equations and turbulent model, study has been carried out in the fluid and solid regions by FVM. The diffusion term is approximated by a first-order central difference formula in momentum and energy equations that provides a stable solution, and the second-order upwind separation scheme has been used for convective terms. In order to solve the flow field, the SIMPLE algorithm [31–35] has been employed, which is an iterative method. The calculation is initialized by defining the pressure field and, the velocity components have been implemented to solve the momentum equation. From the Fig. 2a, it is clearly seen that after 20, 000 N_e , the trend of C_p becomes linear and constant, which indicates that 20,000 N_e (Demartini et al. [34] and Saha [37]) are sufficient to carry out the future analysis. Model validation has been done on the same geometrical configuration and boundary conditions as set in the experimental work of Demartini et al. [34], where they

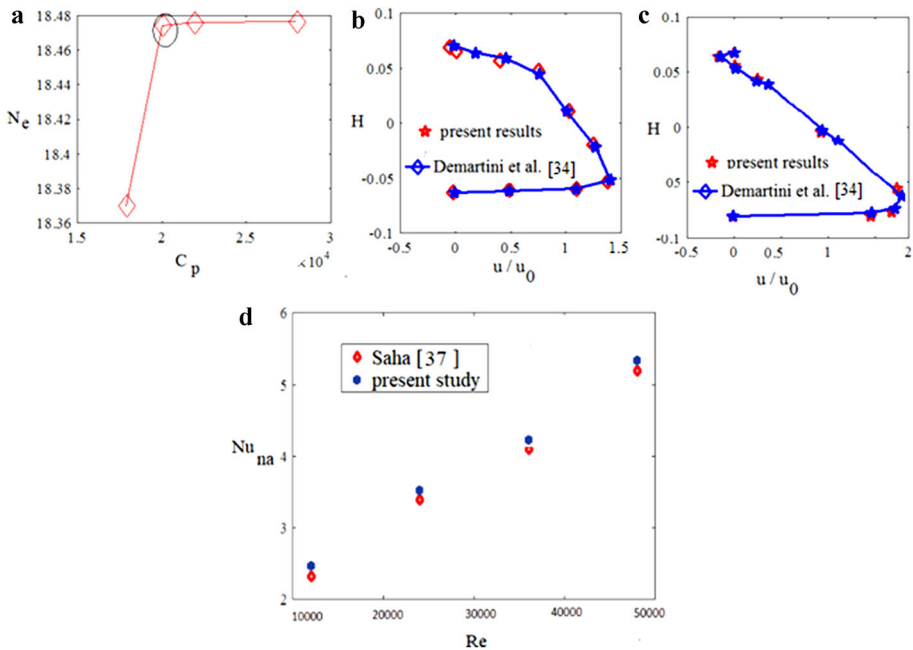


Fig. 2 Plots of **a** C_p vs. N_e and the variations of u/u_0 at **b** $x = 0.159$ m, **c** $x = 0.189$ m and **d** Nu_{na} for different Re

have mounted two plane baffles alternately on the lower and upper walls of the channel. At different locations, and $Re = 87,300$, Fig. 2b–c, present a strong agreement between the result of Demartini et al. [34], and this work. Figure 2d presents the plots of Nu_{na} for different values of Re . The Fig. 2b–d show that the results of this work are too closed to those of Demartini et al. [34] and Saha [37], which provides enough confidence to continue the present study.

Results and Discussion

In this section, different characteristics of flow phenomena and transfer of heat have been presented in the form of graphs.

Flow Characteristics

Streamlines have been shown in Fig. 3a–d, where the first and fourth baffles are detached from the walls and another two baffles are alternately placed on walls. It is observed that the vortices length is influenced by the inter-baffle distance and streamlines are affected by the presence of the first centralized baffle, for which the fluid flow is bifurcated. The two sharp edges are found to form at the upstream; represent the points at which the flow streamlines split, and the cells of recirculation are formed in the upper and lower regions behind the baffle. These rings are formed due to the reduction in the pressure there. Near the first attached baffle, the flow streamlines are synchronized with the reverse fields, where low-intensity recycling areas are formed near the left side of the upper edge of the baffle, while strong recycling cells are formed behind the same baffle. Near the second attached baffle, the flow fields encounter the insulated wall. Consequently, pressure decreases in the base of the baffle due to the formation of a small recirculation zone. In addition, it has been observed that the pressure becomes stronger at the top of the second attached baffle and the flow velocity becomes maximum near the upper portion of the second centralized baffle. Two vortices are formed in the flow field, one is found at the upper right of the second centralized baffle and another one is created near the base of the baffle. From Fig. 3a–d, it is observed that the flow recirculation region becomes more intense with the increase in Re . In the entrance of the channel, pressure reaches its maximum value at the upper and lower edges of the first centralized baffle due to the reduction of flow area, as shown in Fig. 4a–d. Although pressure decreases after the second attached baffle as well as before and after the second detached baffle, it is observed that stream goes downwards due to the collision with the first attached baffle and flow continues to move sharply at the lower part of it. The flow velocity is decreased behind the first detached baffle as well as at the downstream of the second baffle. The velocity of the flow at the top of the second centralized baffle attains its maximum due to the presence of the third baffle, and then decreases because of low pressure at the downstream of the last two baffles.

Profile of Velocity

At different locations, velocity profiles have been shown in Fig. 5a–c. The analysis of velocity profile reveals existence of four flow zones. The first zone is located at the upstream of the first detached baffle, where the flow reaches with constant velocity and the second zone is located in the region between first detached baffle and first attach baffle, while the third and

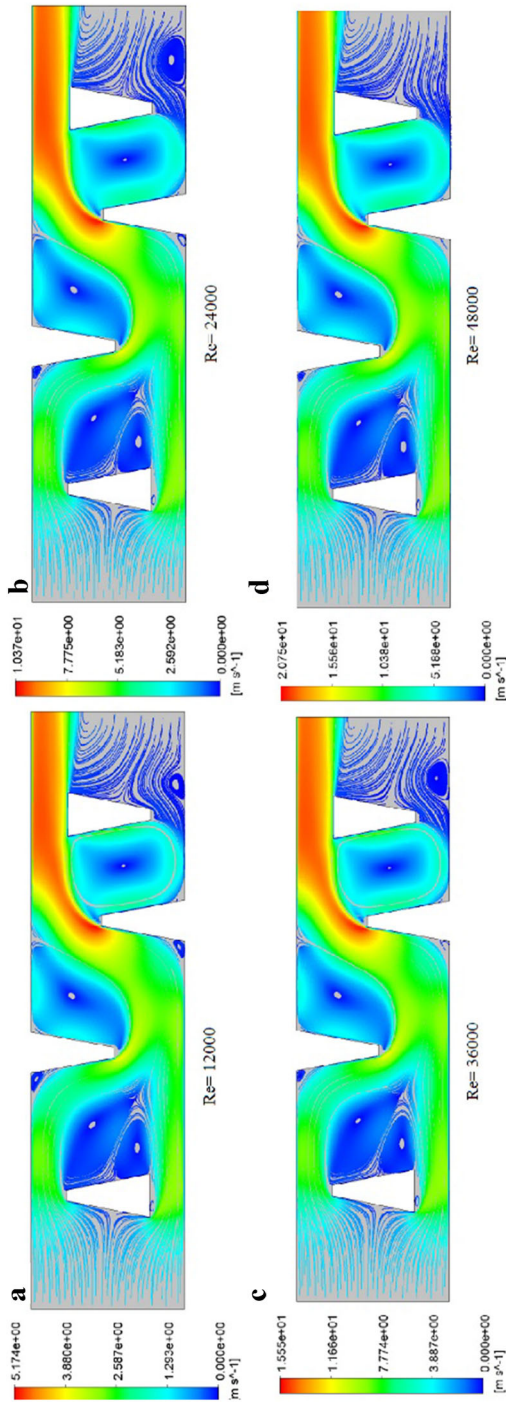


Fig. 3 Velocity streamlines at **a** Re = 12,000, **b** Re = 24,000, **c** Re = 36,000 and **d** Re = 48,000

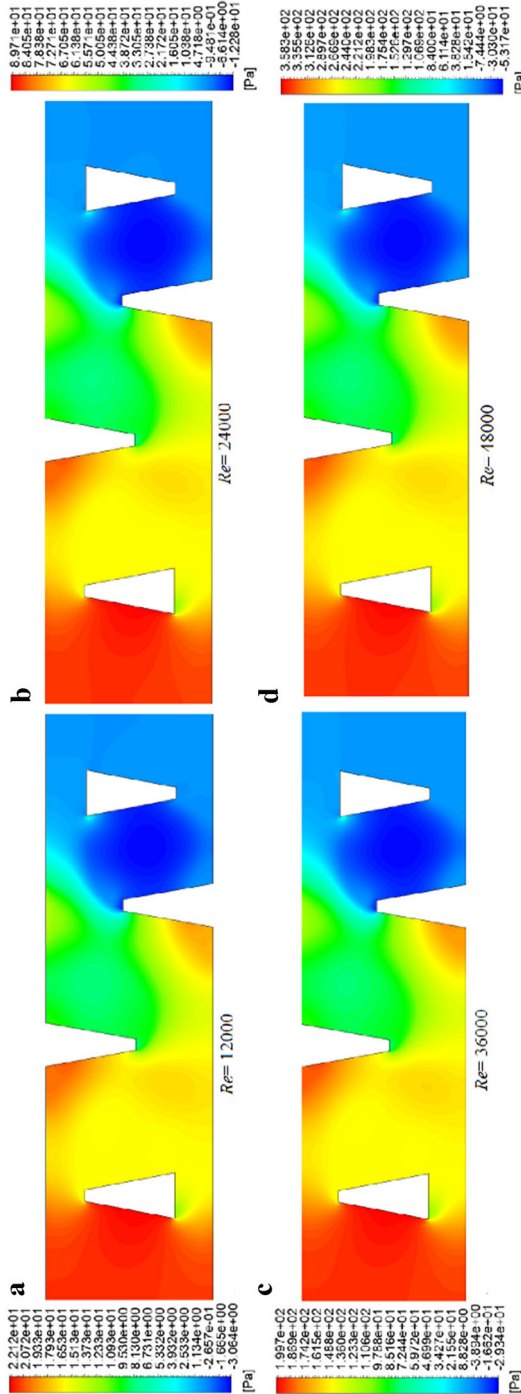


Fig. 4 Pressure contours at **a** $Re = 12,000$, **b** $Re = 24,000$, **c** $Re = 36,000$ and **d** $Re = 48,000$

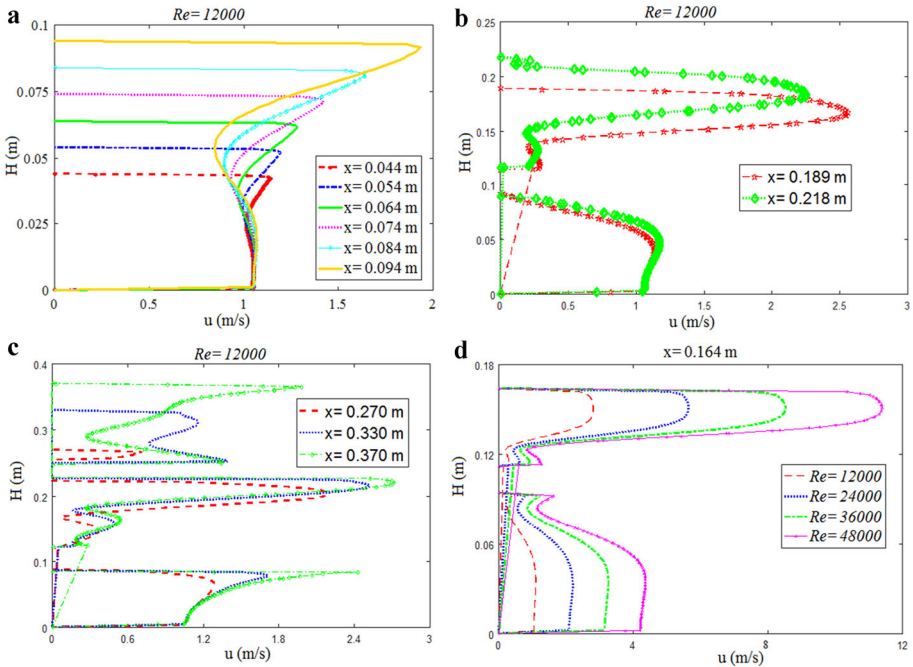


Fig. 5 Variations of velocity plot at **a–c** different locations, variation of **d** u (m/s) for various Re

fourth zones are formed after the first attached baffle and before the second centralized baffle respectively. Due to the presence of baffles a vortex is formed, which affects not only the flow fields but also the size of the primary vortex, and the resistance in the flow offered by the baffle causes the formation of weak zones. It is observed from the Fig. 5a, as the flow approaches to the first baffle the flow streams are deflected, which causes the decrease in axial velocity. It is also found that due to significant reduction inflow area and high-pressure, maximum velocity attained at the lower and upper portion of the first centralized baffle. Figure 5b shows the variation in the axial velocity at two locations after the first centralized baffle. Because of the reduction inflow area, pressure increases near the first attached baffle. At $x = 0.218$ m, $x = 0.370$ m and at $Re = 12,000$, flow velocity becomes approximately 2.25 times and 2.75 times of inlet velocity respectively as shown in Fig. 5a and 5b. Moreover, the profiles of axial velocity have been shown at $x = 0.270$ m, 0.330 m and 0.370 m, which are located between first attached and second attached baffles (Fig. 5c). Figure 5d shows the variations of axial velocity at $x = 0.164$ m for various $Re \in [1–12, 12–37]$. Furthermore, it is also found that at $x = 0.164$ axial velocity becomes 1.7 times and 11.22 times of inlet velocity at $Re = 12,000$, $48,000$ respectively. Therefore, it is clear that axial velocity becomes more pronounced with the increase in Re .

Thermal Behaviour

Detail analysis of heat transfer characteristics, such as $NC_f(x)$, F , $Nu(x)$ and Nu_{av} have been discussed in the following subsections.

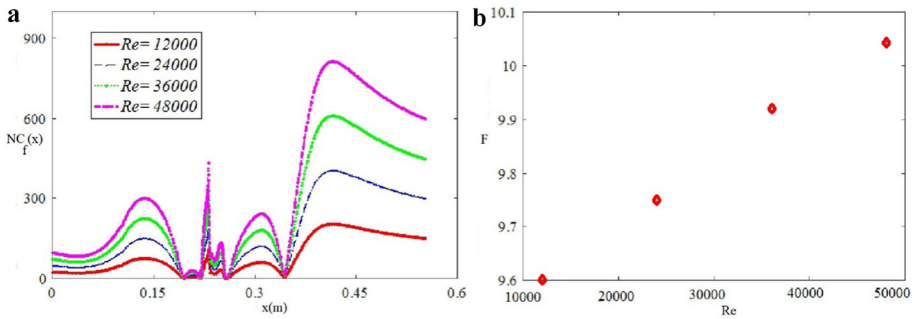


Fig. 6 Plots of **a** $NC_f(x)$ at different locations, **b** F for various Re

Distribution of $C_f(x)$

For the enhancement of heat exchange, the presence of baffles is important. Generally, the friction coefficient leads to the increase in pressure drop. Along the hot wall, Fig. 6a shows the variations in $NC_f(x)$ for various Re . It is observed that friction values are almost constant during the flow of the fluid through the horizontal axis and found to be increased gradually as the flow approaches towards the upper portion of the first centralized baffle. Moreover, due to the presence of a recirculation zone, the $NC_f(x)$ values become higher after the first detached baffle that makes the flow towards the hot wall, and causes increase in the values of $NC_f(x)$. Due to presence of first attached baffle, the value of $NC_f(x)$ gradually decreases, and the flow moves towards downward. It is found that $NC_f(x)$ increases after the first attached baffle due to the formation of weak zones. It has been observed that the values of $NC_f(x)$ decreases rapidly due to the formation of large vortices near the tip of the baffles. It is also observed that the value of $NC_f(x)$ increases at the locations corresponding to the recirculation zone. It is also observed that the values of $NC_f(x)$ increases very significantly at the upper portion of the second attached baffle, as a result, flow velocity attains its maximum, and the same decreases sharply after the last baffle due to the reduction in contact area between the flow and the hot wall surface. In addition, highest $NC_f(x)$ values are observed at the tip of the baffle, i.e., at an area of highest turbulent intensity. Moreover, it is investigated that due to the presence of four baffles, four peaks are observed. From the Fig. 6a, it has been found that the highest $NC_f(x)$ value attains after the approximate axial location 0.32 m, as it lies between the second attached baffle and third attached baffle. From the streamline figures, we see that after crossing the second attached baffle, fluid flows smoothly towards the third baffle. However, the third baffle does not allow the fluid to flow smoothly. It strikes the tip of the baffle, and the values of $NC_f(x)$ increases. Again, we see that the value of $NC_f(x)$ decreases, as after crossing the third baffle the flow strikes the upper wall before moving towards the fourth baffle. With the increase value of Re , it has been found that the value of F increases due to the increase in pressure drop.

Distribution of Nusselt Number

Figure 7a presents the distribution of Nusselt number along the hot wall for different values of Re . In the downstream section, due to formation of vortices there exists a big jump in the values of $Nu(x)$. It is found that the increase in Re causes increase in the values of Nu_{av} , and the $Nu(x)$ distribution becomes more pronounced with the increase in Re as shown in Fig. 7a. It is

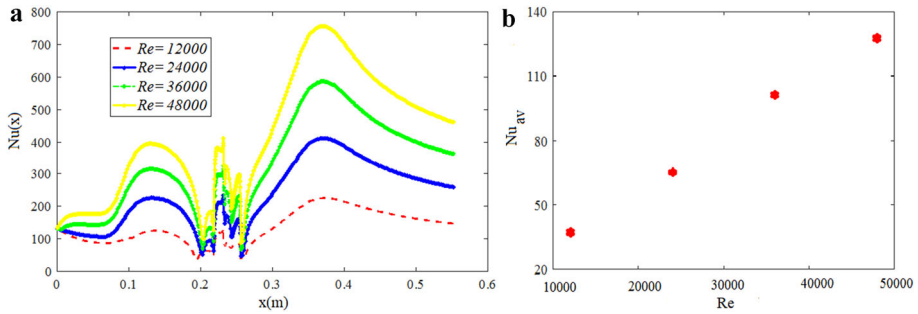


Fig. 7 Plots of **a** $Nu(x)$ versus x (m), **b** Nu_{av} for various Re

also studied that the heat transfer rate is increased near hot wall, and the first attached baffle. Thermal gradient increases near the first attached baffle, which causes significant increase in the values of heat exchange and energy. After the first attached baffle, heat transfer rate is increased due to increase in the recirculation length, which causes the thermal exchange. However, the heat exchange rate decreases as the fluid flow towards the second attached baffle. With the increase in the value of Re , thermal gradient increases, this causes the recirculation length to become more intense. In the Fig. 7b, it has been demonstrated that the values of Nu_{av} increases with the increase in Re . It is observed that the value of $Nu(x)$ goes on increasing and attains its maximum at the baffle tip, and the heat transfer rate attains its maximum at the base of the baffles. The results show that the value of Re and turbulence rise as long as the flow velocity or acceleration increases, as a result heat dissipation increases. The temperature of the flow rises in the inter-baffle region, which means that the presence of baffles causes dissipation of heat from the walls of the channel, which enhances the HT.

Conclusions

Baffles are used in shell and tube of heat exchanger models and in various engineering applications, where the characteristics of thermal behavior and flow phenomena are needed to be identified. The concluding remarks on this work are as follows:

- It is noted that the flow recirculation region becomes more intense with an increase in Re . It has been investigated that friction value increase after the first attached baffle due to the formation of weak zones and the values of friction factor increases as Re increases.
- At $x = 0.218$ m, 0.370 m and at $Re = 12,000$, flow velocity reaches approximately 2.25 times and 2.75 times of inflow velocity respectively. Furthermore, it is also investigated that at $x = 0.164$ m, axial velocity reaches 1.7 times of inflow velocity for $Re = 12,000$, while it becomes 11.22 times of inflow velocity for $Re = 48,000$. Therefore, it is clear that axial velocity becomes more pronounced with the increase in Re .
- It is revealed that the increase in the values of Re causes the increase of average Nusselt number. The present simulation results will help to design, and monitor flows of many thermal applications.

Acknowledgements The authors wish to thank the reviewers for their valuable suggestions, which helped a lot to improve this work.

Funding None.

Data Availability Enquiries about data availability should be directed to the authors.

Declarations

Conflict of interest The authors declares that they have no conflict of interest.

References

- Petukhov, B.: Heat transfer and friction in turbulent pipe flow with variable physical properties. *Adv Heat Tranf* **6**, 503–564 (1970)
- Dittus, W.F., Boelter, M.L.K.: Heat transfer in automobile radiators of the tubular type. *Int. Commun. Heat Mass Transf.* **12**(1), 03–22 (1985)
- Wiemer, P.: Untersuchungber den Zugwiderstand von Wasserrohrkesseln. Dissertation, RWTH Aachen (1937)
- Gunter, A.Y., Sennstrom, H.R., Kopp, S.: A study of flow patterns in baffled heat exchangers. *ASME*, 47-A-103 (1947)
- Bergelin, O.P., Brown, G.A., Colburn, A.P.: Heat transfer and fluid friction during flow across banks of tubes-V: a study of a cylindrical baffles exchanger without internal leakage. *ASME J. Heat Transf.* **75**, 841–850 (1953)
- Gay, B., Williams, T.A.: Heat transfer on the shell-side of a cylindrical shelland-tube heat exchanger fitted with segmental baffles. *Transf. Ins. Chem. Eng.* **46**, 95–100 (1968)
- Gay, B., Mackley, N.V., Jenkins, J.D.: Heat transfer in baffled cylindrical shell-and-tube exchangers: an electrochemical transfer modelling technique. *Int. J. Heat Mass Transf.* **19**(9), 995–1002 (1976)
- Gay, B., Jenkins, J.D., Mackley, N.V.: Shell-side heat transfer coefficient in cylindrical heat exchangers: the influence of geometrical factors, I. The leakage case. *Lett. Heat and Mass Transf.* **4**, 41–52 (1977)
- Gay, B., Jenkins, J.D., Mackley, N.V.: Shell-side heat transfer coefficients in cylindrical heat exchangers: the influence of geometrical factors. *Lett. Heat and Mass Transf.* **8**(6), 437–452 (1981)
- Patankar, S.V., Liu, C.H., Sparrow, E.M.: Analysis of laminar forced convection heat transfer in ducts. *J. Heat Transf.* (1977)
- Berner, C., Durst, F., McEligot, D.M.: Flow around baffles. *J. Heat Transf.* **106**, 743–749 (1984)
- Webb, G.W., Ramadhyani, S.: Fluid flow and heat transfer in a parallel platechannel with staggered baffles. *J. Heat Mass Transf.* **28**(5), 471–495 (1985)
- Webb, B.W., Ramadhyani, S.: Conjugate heat transfer in a channel with staggered ribs. *Int. J. Heat and Mass Transf.* **28**(9), 1679–1687 (1985)
- Habib, M.A., Attya, A.E., McEligot, D.M.: Calculation of turbulent flow and heattransfer in channels withstreamwise-periodic flow. *ASME J. Turbomach.* **110**, 405–411 (1988)
- Habib, M.A., Mobarak, A.M., Sallak, M.A., Hadi, E.A., Affy, R.I.: Experimental investigation of heat transfer and flow over Ba_es of Di_erent heights. *J. Heat Transf.* **116**, 1609–1617 (1994)
- Al-Atabi, M.T., Chin, S.B., Luo, X.Y.: Visualization of mixing of flow in circular tubes with segmental baffles. *J. Vis.* **8**(2), 89–92 (2005)
- Al-Atabi, M.T., Chin, S.B., Luo, X.Y.: Flow structure in circular tubes withsegmental baffles. *J. Vis. Image Process* **12**, 301–311 (2005)
- Bazdidi, F., Naderi, M.: Numerical analysis of laminar heat transfer in entrance region of a horizontal channel with transverse fins. *Int. Commun. Heat Mass Transf.* **31**, 211–220 (2004)
- Kelkar, K.M., Patankar, S.V.: Numerical prediction of flow and heat transfer in a parallel plate channel with staggered fins. *J. Heat Transf.* **109**, 25–30 (1987)
- Prusty, P., Rout, S., Barik, K.A.: Heat transfer correlation for a triangular protruded surface with a cross-flow jet. *Sadhana* **44**(5), 1–14 (2019)
- Saha, S., Biswas, P., Nath, S., Singh, L.: Numerical simulations of Newtonian fluid flow through a suddenly contracted rectangular channel with two different types of baffle plates. *Soft Comput.* **25**, 9873–9885 (2021)
- Chhanda, S.N., Barik, K.A.: Conjugate heat transfer in a rectangular channel with perforated protrusion and cross-flow effect. *Int. J. Control Theory Appl.* **10**(6), 91–100 (2017)
- Barik, K.A., Rout, S., Mukherjee, A.: Numerical investigation of heat transfer enhancement from a protruded surface by cross-flow jet using Al_2O_3 nanofluid. *Int. J. Heat Mass Transf.* **110**, 550–561 (2016)

24. Prithviraj, M., Andrews, M.J.: Three dimensional numerical simulation of shell and tube heat exchangers. *J. Numer. Heat Transf.* **33**(6), 799–816 (1988)
25. Prashanta, D., Akram, H.: Internal cooling augmentation in rectangular channel using inclined baffle plates. *Int J. Heat Fluid Flow* **26**, 799–816 (2005)
26. Shivani, T., Gajusingh, A., Nasiruddin, S., Kamran, S.: The impact of a vortex induced by a baffle on the turbulent structure. *Exp. Therm. Fluid Sci.* **34**, 590–602 (2010)
27. Kang, K., Anand, N.K.: Use of porous baffles to enhance heat transfer in a rectangular channel. *Int. J. Heat Mass Transf.* **46**(22), 4191–4199 (2003)
28. Behera, P.P., Barik, K.A., Malik, K.R.: Heat transfer enhancement for a trapezoidal protruded surface with cross-flow jet. *Int. J. Control Theory Appl.* **10**(6), 449–459 (2017)
29. Karwa, R., Maheshwari, K.B., Karwa, N.: Experimental study of heat transfer enhancement in an asymmetrically heated rectangular duct with perforated baffles. *Int. Commun. Heat Mass Transf.* **32**, 275–284 (2005)
30. Bhuiya, K.K.M., Chowdhury, U.S.M., Saha, M., Islam, T.M.: Heat transfer and friction factor characteristics in turbulent flow through a tube fitted with perforated twisted tape inserts. *Int. Commun. Heat Mass Transf.* **46**, 49–57 (2013)
31. Barik, K.A., Mukherjee, A., Patro, P.: Heat transfer enhancement from a small rectangular channel with different surface protrusions by a turbulent cross flow jet. *Int. J. Therm. Sci.* **98**, 32–41 (2015)
32. Mukherjee, A., Rout, S., Barik, K.A.: Heat transfer and entropy generation analysis of a protruded surface in presence of a cross-flow jet using Al_2O_3 -water nanofluid. *Therm. Sci. Eng. Prog.* **5**, 327–338 (2015)
33. Mukherjee, A., Barik, A.: Heat transfer enhancement from a ribbed surface in presence of a cross flow jet: a numerical investigation. *J. Mater. Sci. Mech. Eng.* **3**(3), 172–178 (2016)
34. Demartini, L.C., Vielmo, H.A., Miller, S.V.: Numeric and experimental analysis of the turbulent flow through a channel with baffle plates. *J. Braz. Soc. Mech. Sci. Eng.* **26**(2), 153–159 (2004)
35. Nasiruddin, M.H., Siddiqui, K.: Heat transfer augmentation in a heat exchanger tube using a baffle. *Int. J. Heat Fluid Flow* **28**(2), 318–328 (2007)
36. Launder, B.E., Spalding, D.B.: The numerical computation of turbulence. *Comput. Methods Appl. Mech. Eng.* **3**(2), 269–289 (1974)
37. Saha, S.: Numerical simulation of turbulent airflow and heat transfer through a rectangular channel along with trapezoidal baffle plates. *AIP Conf. Proc.* **2341**, 1–10 (2021)

Publisher's Note Springer Nature remains neutral with regard to jurisdictional claims in published maps and institutional affiliations.